Analyses of stone surfaces by optical methods

Tantussi G.[1] and Lanzetta M.[1, 2]
[1] University of Pisa, Department of Mechanical, Nuclear and Production Engineering (DIMNP), Via Bonanno Pisano, 25/B, 56126 Pisa, Italy, (tantussi, lanzetta)@ing.unipi.it
[2] National Research Council (CNR), Institute of Information Science and Technologies (ISTI) "A. Faedo", Via G. Moruzzi, 1, 56124 Pisa, Italy

Abstract

Ornamental stone products are generally used for decorative cladding. A major quality parameter is their aesthetical appearance, which directly impacts their commercial value. The surface quality of stone products depends on the presence of defects both due to the unpredictability of natural materials and to the actual manufacturing process.
This work starts reviewing the literature about optical methods for stone surface inspection. A classification is then proposed focusing on their industrial applicability in order to provide a guideline for future investigations.
Three innovative systems are proposed and described in details: a vision system, an optical profilometer and a reflectometer for the inspection of polished, bush-hammered, sand-blasted, flame-finished, waterjet processed, and laser engraved surfaces.

Keywords: ornamental stone, texture analysis, visual inspection, surface quality

1 INTRODUCTION

Ornamental stone products are generally used for decorative cladding. A major quality parameter is their surface aesthetical appearance, which directly impacts their commercial value.
The surface quality of stone products depends on the presence of defects both due to the unpredictability of natural materials and to the actual manufacturing process [1].
In addition to aesthetical examination (*inspection*) [2] [3] [4] [5] [6], optical methods are able to analyze the surface as a result of a manufacturing process (process control).
Considering the relatively low innovation, technological and automation level, most control operations in the stone industry are carried out manually. However the developed countries will need to improve the quality of products and the automation level to maintain their production alive and competitive in a global or even in a local market.
Surface analysis has been extensively reviewed by authors [7] [8] [9], including optical approaches [10] [11] [12] [13], but very few papers deal with stone surfaces [14] [15]

[16], particularly using optical methods [17] [18].
It seems that the potential of optical analyses is able to cover most surface inspection needs. This will be demonstrated by proposing a classification of surface types and an optical inspection method for each class.
In the first part of the paper (§ 2 to 5) we will review the four optical methods outlined in Figure 1, which have been selected for their capability of covering the full inspection range of stone manufactures, as shown in the second part of the paper (§ 6).

1.1 Classification of stone surfaces

Our work is based on the hypothesis that the result of stone surface processing can be univocally assessed by examining the surface topology.

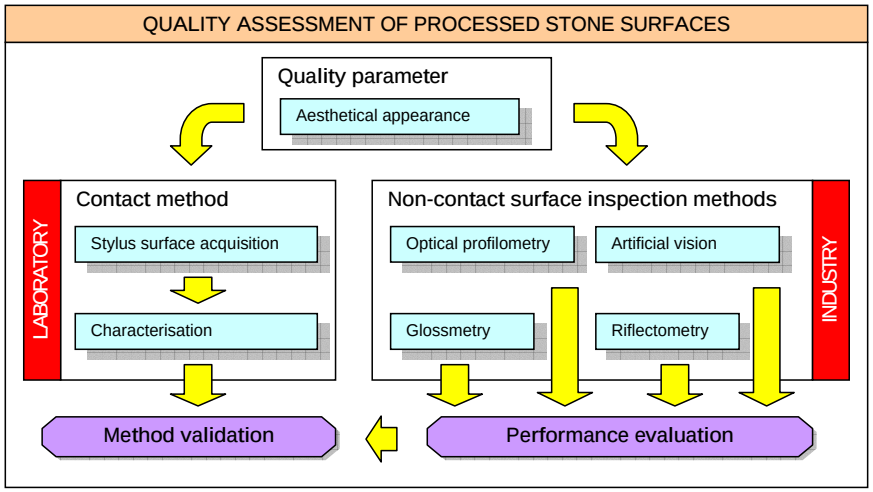

Figure 1. Correlation between surface and optical properties of stone products.

This work examines plane products, such as slabs, tiles and mosaics with different surface finish grade.
The order of magnitude of the average surface features in commercial products can be as low as Ra = 0.01 μm [19] with waviness Wt less than 0.2 μm in the case of polished slabs or tiles and reach peak valley differences Pt for the primary profiles in the order of few millimeters in the case of bush-hammering, sand-blasting, flame-finishing, carving or waterjet processing.
Based on the optical methods reviewed in this paper, we classify the amplitude range of the examined stone surfaces in three groups in terms of Ra and Pt (difference in level between the highest peak and the lowest valley in a random primary profile sample, with negligible errors of form).

The lower and upper bound of the proposed classification, are

- *smooth* surfaces: Ra < 1 μm
- *rugged* surfaces: Pt > 100 μm

and by difference, it also includes an intermediate group that we will call *rough* surfaces (e.g. semi-finished products).
The evaluation length will depend on the sampling length, which is

- the standard 0.8 mm for smooth surfaces, or lower if required and
- 2.5 mm for rugged surfaces.

The presence of markings or engravings for decoration or identification purposes will also be included in the classification, and belong to the rugged surfaces class, due to the size of features.

2 GLOSSMETRY

Current industrial practice in the inspection of Marble, Granite and other ornamental polished stone surfaces is the gloss measurement by a glossmeter (or scatterometer). Such photoelectronic instrument is imported from different industrial fields, for the gloss measurement [20] [21] of metal surfaces [22], paints and varnishes [23], ceramics [24] [25], etc. It measures the amount of light directed and reflected at a defined angle, by integrating the total scatter (reflected and diffused light).

2.1 Standard gloss measurement

In the standard measurement procedure, the gloss value is given by the ratio of two terms:

- the luminous flux reflected into a given diaphragm centered on the specular direction at the surface of the specimen and
- the luminous flux reflected, in the same conditions, on the surface of a standard plane glass.

Both are measured by a receptor at corresponding angles of specular reflection.
The measurement scale is expressed in Gloss Units (GU) in a range between 0 and 100. The gloss values measured with this method must be calibrated against a standardized reference value in order to correlate values obtained by standard methods. In the instrument calibration phase [20] a specular gloss value of 100 is assigned to a highly polished, plane, black glass with a refractive value of 1.567. The gloss value of glass with different refractive index can be computed from the Fresnel equation [26]. The gloss values can be higher than 100 for surfaces that reflect more than the reference surface.
The standard angles of incidence are 20°, 45°, 60°, 75° and 85° (with respect to an axis perpendicular to the measured surface). The most suitable geometry for general applications is 60^{o}. The best optical geometry for surface with very high and very low gloss is respectively 20° and 85°.

2.2 Standard gloss measurement of stone surfaces

The gloss of some polished stone surfaces can be higher than 100 GU.
The main benefits of commercial glossmeters are their relatively low cost and their ability to quickly take gloss measurements, which are accurate enough for current stone market needs. The main drawbacks are that they only work on very smooth surfaces so they have limited application to the last polishing stages, with Ra lower than 1 μm and cannot be used for process control in other process phases.
The main features and limitations of glossmeters for application in stone analyses have been systematically investigated and will be discussed in a future publication. In extreme synthesis, glossmeters are deceived by the retransmitted light component, which may be relevant for translucent materials (like stones) and which vary for different stone types. For this reason, measurements are consistent if taken under the same conditions, particularly optical geometry and material, but measurements may also be influenced by the inherent variability of a natural material.
The practical implication of the above, is that each individual material being polished (and usually many are processed on a production line every day) requires the definition of a correlation with roughness, a complex operation to be carried out in a clean, separate environment by skilled operators, and none of these conditions is satisfied by most stone companies.
As a result, although present in most companies, glossmeters are not really used and manual examination is preferred.

3 REFLECTOMETRY

The interaction between light and surfaces under a theoretical viewpoint has been extensively studied over the last centuries and there is wide recent literature, such as [27] [28]. The application in manufacture in general still poses several problems [29].
Reflectometery offers benefits, which have not yet been exploited in the stone industry [26] [30].
The (specular) Reflectance R_s is the ratio between the intensity of the specularly reflect light I_s and the intensity of the total incident light I_t, as described by the Fresnel equation [26]:

$$R_s(\theta,n) = \frac{I_s}{I_t}$$

The Reflectance is mainly affected by the material properties (refraction index n at the given wavelength λ) and the measuring instrument configuration (angle of incidence of the light ray θ) in addition to the surface roughness (Rq):

$$\frac{I_s}{I_t} = e^{-\left(\frac{4\pi Rq\cos\theta}{\lambda}\right)^2}$$

This expression suggests that higher λ yields higher instrument sensitivity.
Increasing λ also increases the range of measurable roughness at higher roughness, according to the Rayleigh criterion.
To overcome the limitations of glossmeters, two new methods are proposed to directly measure just the reflected component of an incident light (Reflectance) instead of the gloss, which also includes the scattered light.
One of the two systems is based on a CCD camera to measure the amount of specularly reflected light. For the type and method of analysis, this can be considered an artificial vision system for the measurement of Reflectance.
The other system is based on a near infrared (NIR) beam profiler detector.
The preliminary results of this work are reported in § 6.2 and will be discussed more extensively in future publications.

4 ARTIFICIAL VISION SYSTEMS

Over a decade has passed since presentation of the first automated systems able to replace operators in checking the quality of stone manufactures (tiles or slabs): artificial vision systems [4] [5] [6]. Artificial vision is a good solution to color inspection problems [31] [32]. At the Aitem conference [2] [3] and at the exhibition of Carrara the University of Pisa devised several pioneering vision prototypes capable of inspecting stone, while a number of international companies tried to propose them industrially. Despite widespread interest, still alive, application of these systems has been limited to isolated cases, satisfying the following conditions:

- massive production
- low end
- consistency of material type

Among the reasons for a negligible penetration of artificial vision systems in the stone industry are:

- performance inferior to expectation
- high costs, considering average stone company size
- higher technological level than current installations and operator skills, and consequent vulnerability

Historically, similar systems have been successfully proposed in the ceramic production, which in facts takes advantage of higher productivity and investments. If we want to push a little further the analysis of the specifications of visual inspection systems for the stone and the ceramic manufacturing industry, this latter requires higher inspection speed and color discrimination ability, which can be more and more easily achieved with modern processors and sensors respectively (*defect detection*).

The main criticality of artificial vision systems is instead their ability to recognize morphological defects and to classify different morphologies (*classification*) in addition to defect detection.
This requires the identification and formalization of objective criteria, only available in the mind of skilled operators.
In the literature, particularly on information science, very many methods are available. An example is given by [33], which presents a bibliography of over 2250 references related to computer vision and image analysis, arranged by subject matter.
The problem of industrial application of this immense heritage is twofold:

- difficulty of implementing inspection algorithms which are sufficiently general purpose for most stone materials or classes, or, alternatively,
- need of reprogramming the inspection system for each new material, which requires capabilities usually not available by artificial vision system integrators.

This difficulty is demonstrated by the fact that not only such inspection systems are not yet available, but also commercial artificial systems yet do not include effective classification functions.
Concerning simpler operations, image acquisition can help testing the effect of the final layout (tiling) [34]. More recently, real industrial systems start facing the market [35]. Especially for large products (slabs), the most crucial stage is faithful image acquisition.

4.1 Stereo vision for stone surface measurement

Stereo vision is effectively used in three dimensional reconstruction, particularly in robotics [36] and can be virtually applied for surface acquisition. However it has serious limitations due to current sensor technology.
Considering the simplest case of a camera with the optical axis perpendicular to the surface, a stereo pair of images can be obtained with parallel relative translation between camera and surface, which can be alternatively achieved by moving the camera or the surface. However the nominal depth resolution that can be achieved with current sensor technology is two or three orders of magnitude higher than that required. Errors coming from further image processing (e.g. camera calibration stereo matching, triangulation) are additional [37].
Active vision, with controlled vergence between cameras, focus, aperture along with calibration data may improve the accuracy in depth recovery [38] [39].
New applications of stereo vision open up in the stone industry for the analysis of rugged surfaces and will be able to take advantage of the positive trend of matrix camera sensor resolution.

4.2 Characterization of rugged surfaces by artificial vision with structured light

The mentioned applications can benefit of (many) artificial techniques that are not suitable for smooth surfaces for insufficient spatial resolution. Figure 2 shows one of such systems.

A set of about 30 specially developed diffraction grids printed on photographic film has been tested in different geometrical configurations in order to project thin, high-contrast light stripes on a sample for the purpose of three dimensional reconstruction. Some experimental results of general interest are reported in Table 1. The angle of the diffraction grid plane with respect to the laser axis can be tilted in order to achieve additional projected geometries.
A qualitative assessment of the contrast level has been visually determined and it has been sufficient for the selection of the optimal configuration among the ones tested. A quantitative expression can however be easily defined, e.g. considering the light

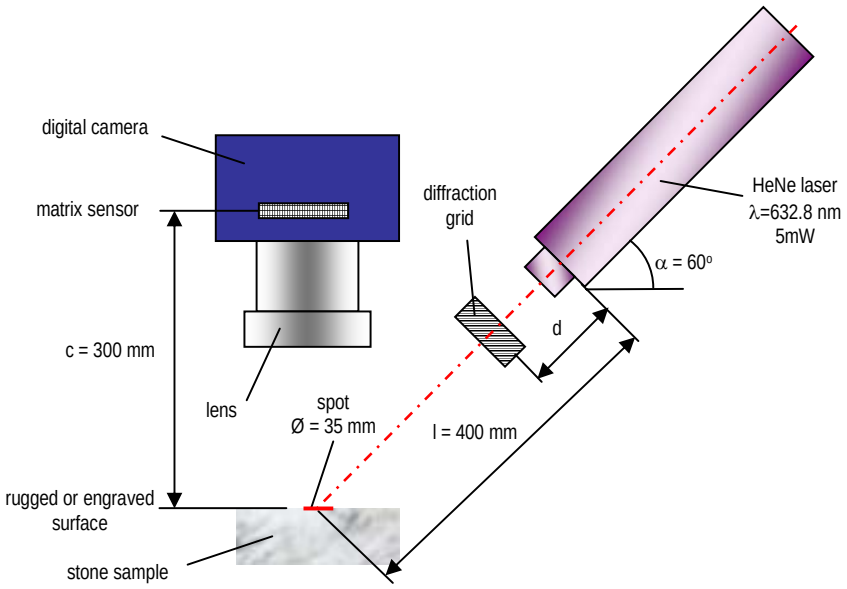

Figure 2. The artificial vision system based on structured light. The values of α, c and l are determined by optical and visibility constraints, considering the small working area; d is reported in Table 1.

intensity of the pixels of the grabbed image I:

$$Contrast = \{Max[I(i, j)]\}/\{Min[I(h, k)]\}$$

where $(i, j) \in \{lines\}$ and $(h, k) \in \{line\ spacing\}$ (Figure 11). *Contrast* ranges between 2 (worst case) and 8 for a 7 or 8-bit images.

4.3 Research perspectives on artificial vision for stone surface measurement

We have presented three new approaches for the analysis of stone surfaces based on artificial vision:

- reflectometry
- stereo vision
- structured light

The typical limitation of sensor resolution makes the last two suitable for the analysis of features in the millimeter range and above (rugged surfaces).
Higher resolution can be achieved integrating multiple techniques [39] [40] [41] [42]

Diffraction grid ID	20	20	20	20	03	03	29	29	23	23	14	14
Diffraction grid line spacing [mm]	0.8	0.8	0.8	0.8	1.1	1.1	1.25	1.25	0.85	0.85	1.7	1.7
Diffraction grid line width [mm]	0.4	0.4	0.4	0.4	0.75	0.75	0.6	0.6	1.6	1.6	0.75	0.75
Diffraction grid – laser distance d [mm]	50	100	150	120	100	70	70	100	100	150	150	100
Projected lines/20 mm	10	17	25	19	24	16	17	-	8	13	13	9
Projected line *width* or spacing [mm]	*1.5*	*1*	1	0.8	1	1.5	1	-	1.5	1.5	1.5	2
Contrast: L=low, M=medium, H=high	L	H	L	L	M	M	L	L	H	M	M	M

Table 1. Comparison among some of the tested configurations of the structured lighting system for the artificial vision system described in Figure 2. The selected configuration is highlighted.

[43] [44] and very many are available in the literature, which have not yet been applied in the stone surface measurement: shadow Moiré [45], depth-from-focus [46], texture analysis [47], scattering [48] approaches, just to cite a few.
Nevertheless, complex instrumentation does not seem to be suitable for the stone industry today for the high research investment required to achieve a sufficient reliability compared to simpler, less accurate, cheaper methods available.

5 OPTICAL PROFILOMETRY

Traditional stylus contact profilometry has well known benefits, such as

- versatility in diversity of shapes, materials and processes,
- high range in resolution in the vertical direction,
- high spatial bandwidth,

but it also has some drawbacks, such as

- accessibility (e.g. deep holes, steep profiles),

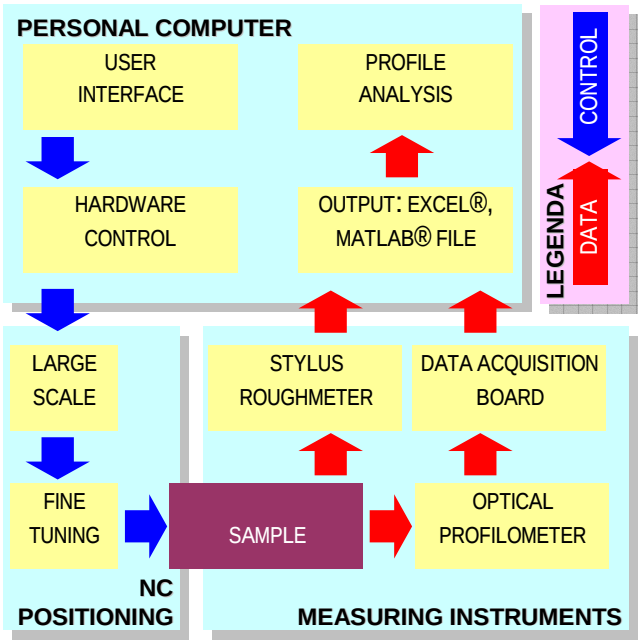

Figure 3. Interactions between the main modules of the developed integrated contact/non-contact surface texture analysis system. The user interface is shown in Figure 4. Details on the main modules are in Table 2.

- the stylus force can in some instances damage the surface or the stylus,
- limitation in the measuring area,
- the technique is relatively low.

The actual instrument may be limited in bandwidth and speed in both cases, however stylus measurement has usually a higher bandwidth and lower speed than optical profilometry.

5.1 Development of an integrated contact/non-contact surface texture analysis system

For the reasons outlined above, we have designed an integrated laboratory system including both a stylus texture measuring instrument and an optical profilometer, in order to overcome the limitations of both methods.
In addition, we take advantage of the higher bandwidth of our stylus instrument to

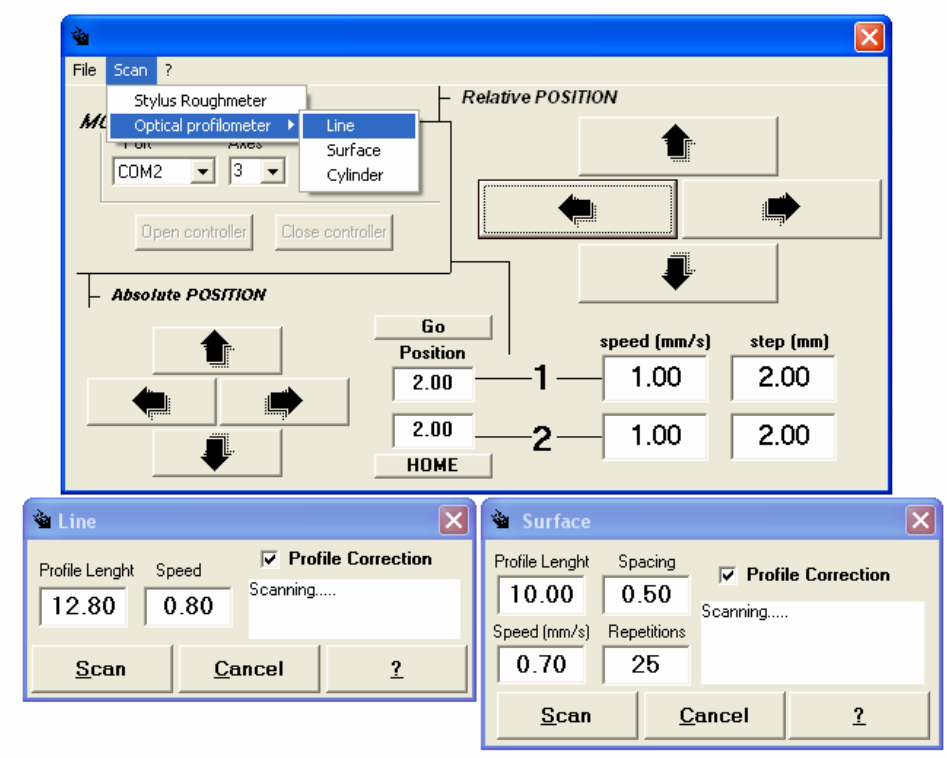

Figure 4. User interface of the control program of the surface acquisition system developed.

validate our optical profilometer, as detailed in § 6.5, according to the scheme of Figure 1, by direct application on a case of industrial interest: the acquisition of rugged surfaces [49] [50] [51].
The logical and data flows of the developed system are shown in Figure 3. The actual components are detailed in Table 2. A view of the software interface with basic acquisition functions is shown in Figure 4.

The commercial optical profilometer used is claimed to be able to measure absolute distances on glass and rubber surfaces. For these extreme capabilities, it has been selected for application on stone surfaces, where the translucent material may pose measurement problems. The working principle is the analysis of the light reception distribution.

6 APPLICATIONS

6.1 Characterization of polished stone surfaces

According to our classification (§ 1.1), polished surfaces belong to the class of smooth stone surfaces.
Current industrial practice in manufacturing polished stone products starts with grinding surfaces with decreasing grain-sized abrasives (usually more than 10 stages) in a consecutive order and is sometimes completed with the application of chemical products to create a film on the smoothened surface to improve brightness. Some stone materials can be polished almost perfectly, depending on the mineral type, crystal size and denseness, cutting direction with respect to crystallization, and fillings in the micro-, macro-discontinuities. Under the measuring viewpoint, chemical reactions and coatings may produce light scattering effects on the surface.
Very few authors have systematically approached the analysis of stone surfaces [15] [16] and most concerning polished surfaces.
This work represents a first systematic and extensive approach to the characterization of stones.
We have examined nine stone types at different polishing stages, among the most common commercial Marble, Granite, Travertine and Breccia.
Some profile examples are shown in Figure 5. It has been clearly observed that most polished surfaces have a plateau like aspect. This is mainly due to the presence of internal porosity, particularly in inhomogeneous materials like granite: the polishing process removes the peaks, but valleys remain unchanged. The most significant exception is travertine, because of the higher magnitude of voids. For this reason we have proposed the use of Rk (DIN 4776) as roughness descriptor.
In addition to being more appropriate, Rk has other benefits:

- it follows the general rule that parameters that are harder to measure are more reliable [13];
- from Figure 6, it can be noticed that the Rk parameter has a larger variation range than Ra and Rq for the polishing stages L6 to L12 and this allows a better discrimination between them;
- from Figure 7, it can be observed that it has a very good correlation with Reflectance in a wide range of roughness, as discussed in the next paragraph.

6.2 Reflectometric analysis of polished surfaces

Component description	Main features related to current application
Stylus surface texture measuring instrument Perthen Perthometer SP3	Standard (ISO, DIN, CNOMO) parameters Gaussian and RC filter Serial (RS 232C) connection to PC (control/data output) Cone stylus, angle: 88º, tip radius: 5 μm
Optical profilometer Omron ZS-LD20T	2D CMOS image sensor Measurement distance: 20 ± 1 mm High-speed sampling: 110 μs Resolution: 0,25 μm Red laser light, spot size: Ø 25 μm Output signal: ± 10 V
Analog/digital acquisition card Labjack U12	USB connection to PC 12-bit resolution Input signal: ± 10 V
NC large scale positioning Motion control card Galil DMC2143 Three controlled axes X-Y screw table, with two stepper motors 1.3 A, 1.8º One rotating axis (for the acquisition of cylindrical surfaces) Supports the fine positioning system	Serial (RS232 at 19.200 bps) connection to PC User-configurable for stepper motors Outputs for stepper motors: up to 3 MHz Position range: 32 bit Theoretical resolution: 0,028° Commands executable by the controller Non-volatile memory for programs and variables Home and limits for each axis 8 TTL uncommitted inputs Communication drivers for Windows® and Visual Basic® development environment
NC fine positioning Translation Stage Pollux VT80 (two stages) Stepper motors 1.2 A, 1.8º Holds the sample	Serial (RS232 at 19.200 Baud) connection to PC Travel range: 100 mm Linear recirculating ball system Limit switches integrated Maximum speed: 20 mm/s Maximum load: 1 kg Repeatability: ± 1 μm, ± 15 μm (bi-directional)

Table 2. The main features of the hardware integrated in the developed surface acquisition system (Figure 3).

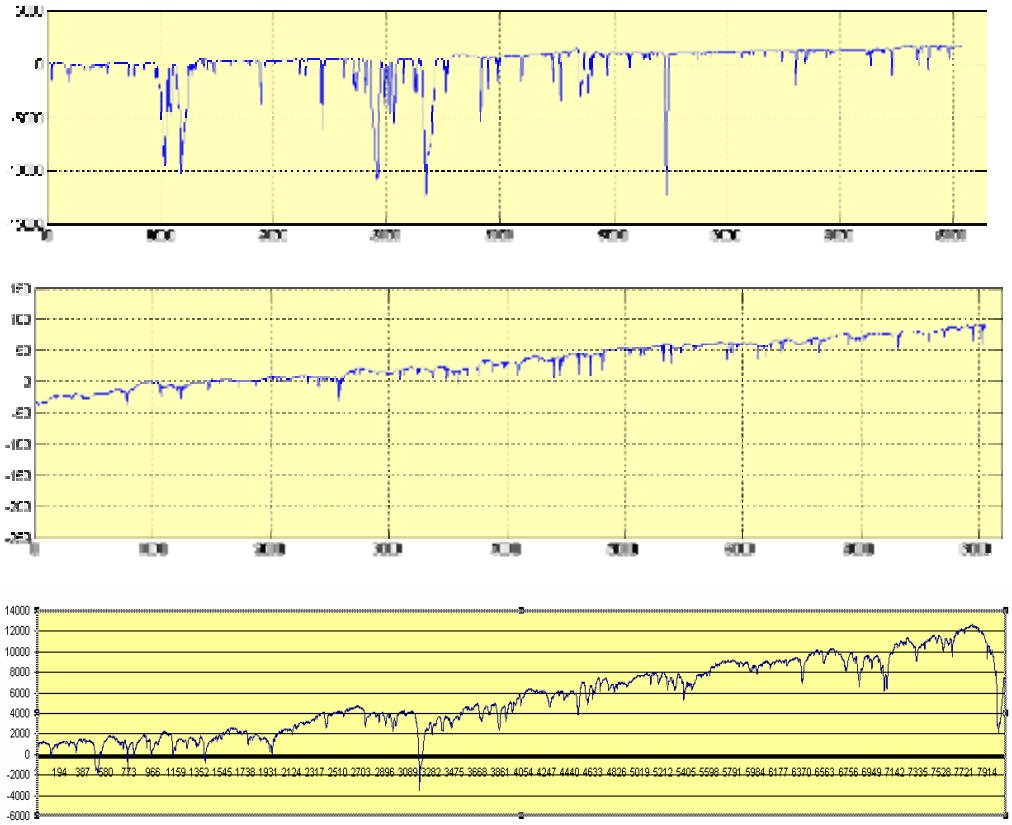

Figure 5. Examples of unfiltered profiles of Granite (top), Marble (center) and Travertine (bottom).

For the design of our innovative reflectometer, a spectrometric analysis of the examined stone has shown the wavelength intervals with higher reflected and diffused components. This has pushed us to the development of two reflectometers, with different light sources and receptors:

1. In our first prototype (artificial vision system), a CCD camera captures a visible HeNe laser ray with wavelength of 633 nm hitting the stone surface at an angle of incidence between 10^{o} and 70^{o}.
2. In our near infrared (NIR) reflectometer prototype, a laser of wavelength 785, 980, 1310 or 1550 nm hits the surface at angles between 10^{o} and 85^{o}. The reflected light is captured by an optical beam profiler.

As shown in Figure 7, the performance of the proposed methods have been experimentally compared in the applications to seven different stone materials with various roughness (Rk between 0.1 and 3 μm).
The correlation between the Reflectance measured by both systems with parameters like Ra, Rq, Rk, Rvk, Rpk, MR1 and MR2 have been examined for the mentioned stone set, showing a very good agreement with the optics theory.
The best configuration of the developed reflectometer has higher incidence angle and wavelength.

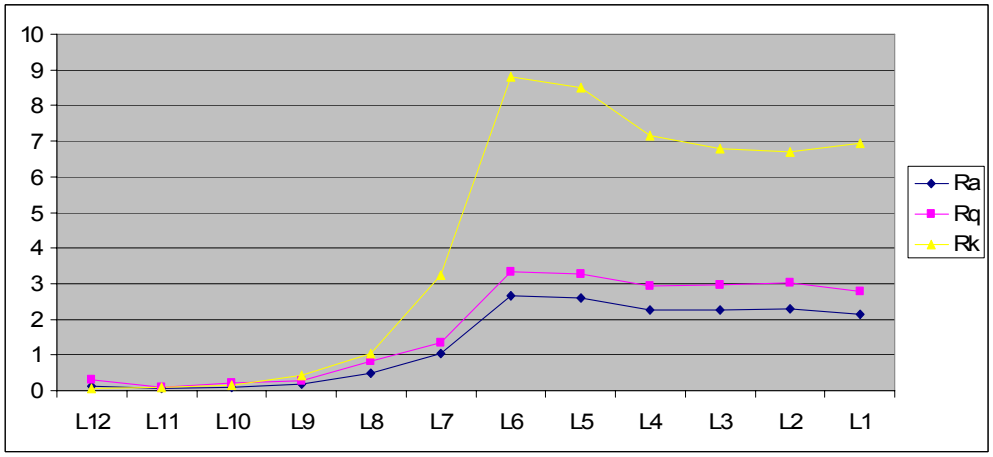

Figure 6. Comparison among Ra, Rq and Rk for a Breccia Sarda at 12 different polishing stages L1 to L12.

By this study a correlation between roughness and incident light has been established by regression (Figure 7) using the most suitable roughness parameter (Rk) describing the stylus measured surface:

$$\frac{I_s}{I_t} = 1.04 - \frac{3.5\cos\theta}{\lambda}\mathrm{Rk} \qquad (1)$$

The extended roughness range, with Rk up to 3 μm, can also be inferred from Figure 7.

6.3 Industrial application of the developed reflectometer

The proposed reflectometer is being patented. Figure 8 shows three industrial exploitation opportunities.

In addition to the research apparatus in two configurations, two engineered reflectometers for manual use have already been delivered.

6.4 Acquisition of rugged surfaces using an artificial vision system with structured light

Engraving is an emerging stone process for identification and traceability (characters or codes) and for decoration (inlay). In § 4.2 we have described a three dimensional artificial vision system, which can be applied for laser- and abrasive waterjet-based engraving. These new processes require the characterization of results for the

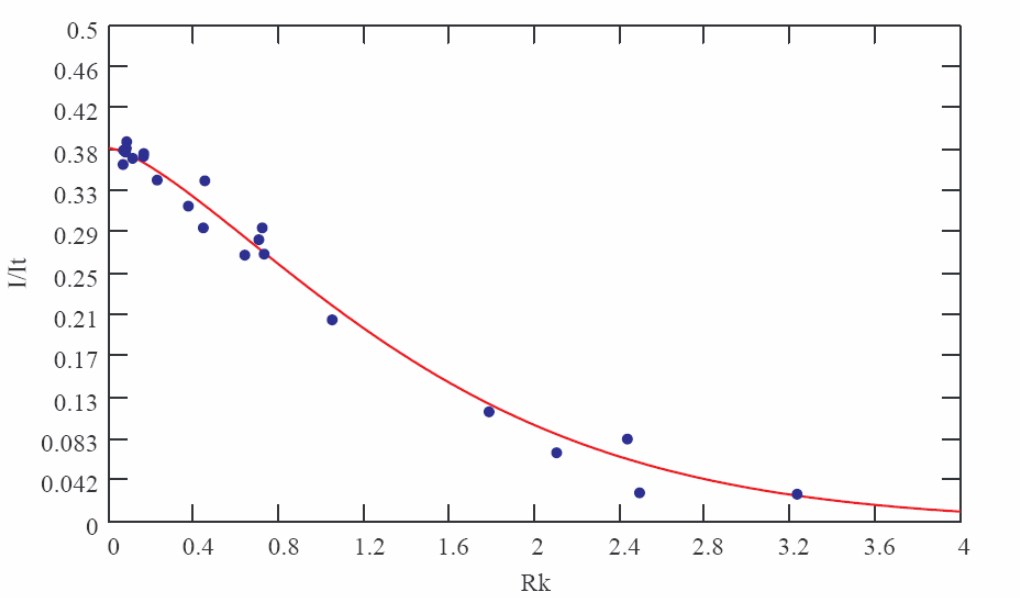

Figure 7. The blue dots show the Reflectance measured by our reflectometer prototype as a function of the (stylus) measured Rk. The red curve has been determined by regression and it has the expression of equation (1) with λ = 1550 nm, θ = 80° and n(λ) = 1.8.

optimization of the technological parameters.

Considering our classification of surfaces (§ 1.1), markings deeper than 100 μm can be approached with the same methods intended for rugged surfaces.

Stylus measurement is not suitable for accessibility reasons and for the risk of damaging the stylus for steep surfaces (shown by the optical profile in Figure 10).

An automatic optical character recognition (OCR) algorithm for the inspection of engraved characters follows the phases in Figure 9.

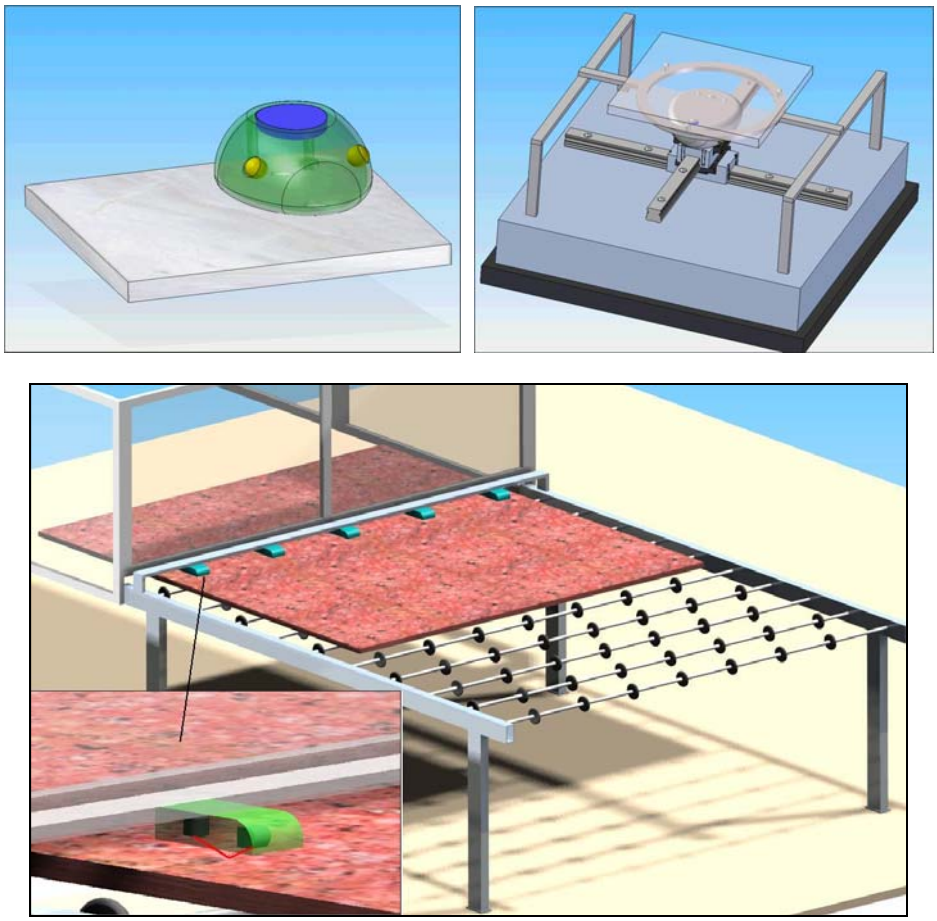

Figure 8. Applications of the developed reflectometer: manual version, mouse-like, sitting on a Marble tile (top, left); laboratory version (top, right), the tile surface, upside down, is referred by three spheres and the reflectometer has a NC movement for multiple acquisition; on-line application of an array of sensors on a Granite slab (bottom).

Most of these phases concern readability issues, for which we can simply rely on available standards. No specific standard is yet available for stone marking, but we can infer the readability requirements from the following:

- [52] and [53] relate to inkjet and similar printing methods. They specify the shapes, dimensions and tolerances for the purposes of character recognition.
- In particular, [54] describes the various types of printing defects and other printing considerations, together with the tolerances permitted, and also

contains specifications for signal level measurement and references to Optical Character Recognition (OCR).

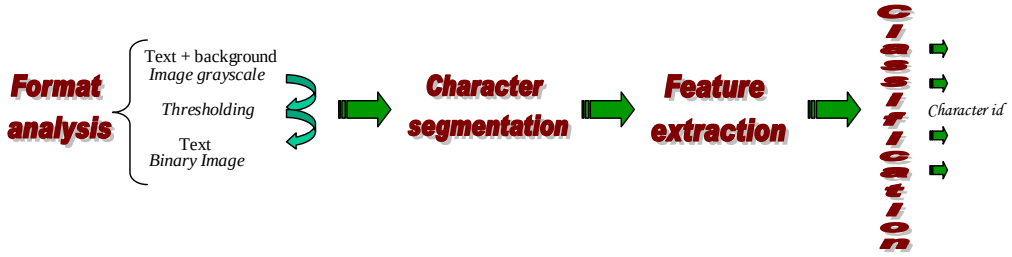

Figure 9. The main steps of automatic Optical Character Recognition (OCR).

The Thresholding algorithm requirements do produce an input for the engraving technology in order to define a correct tool path. Under a manufacturing perspective, we have approached the optimization of the engraving process at two levels:

1. macroscopic, adherence of the actual engraving path to the designed one; this can be simply analyzed by image difference as proposed by Annoni and

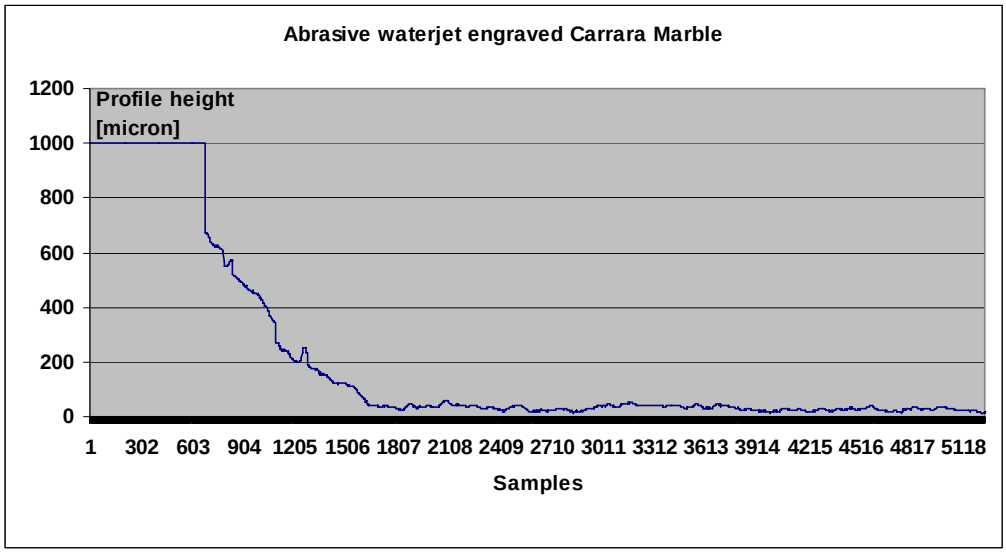

Figure 10. A single surface profile obtained perpendicularly to a marking with the optical profilometer described in Figure 3 with the acquisition parameters in Table 3.

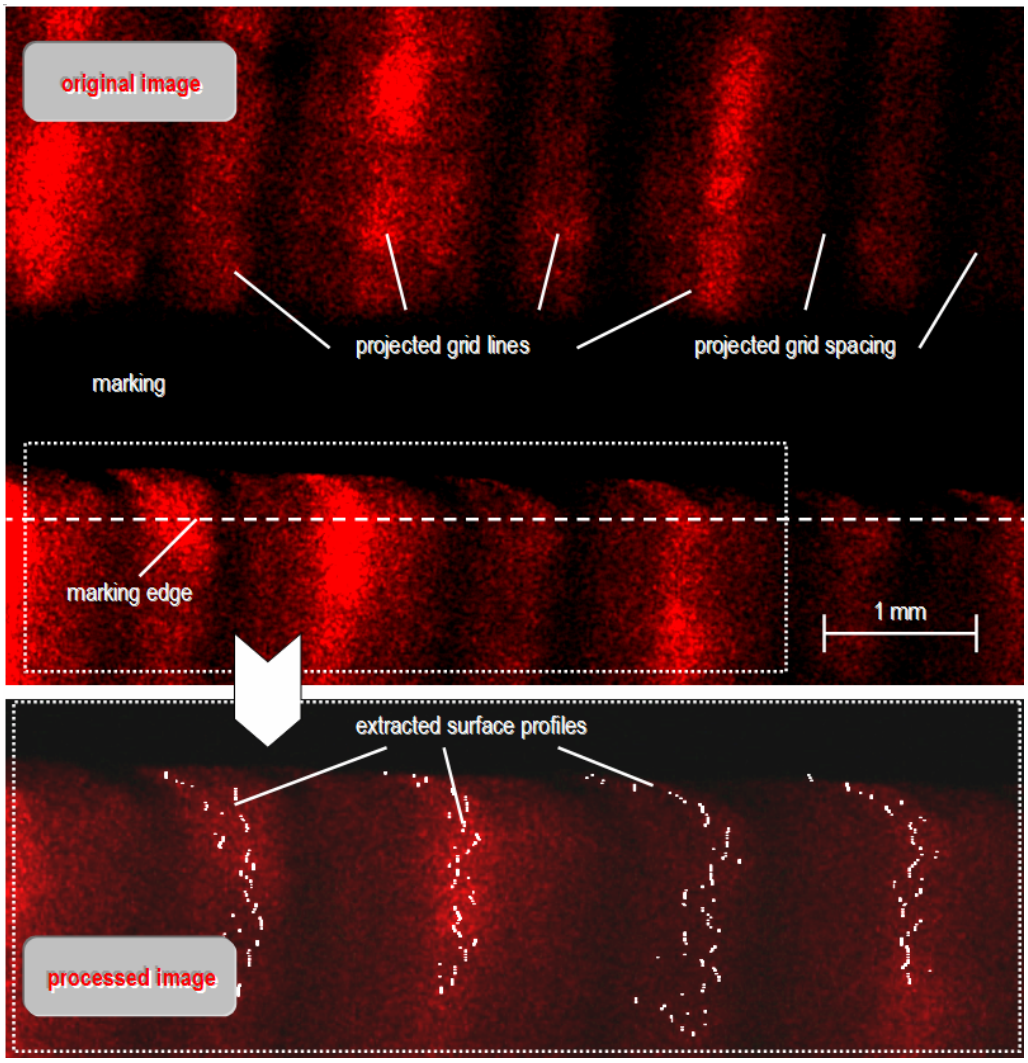

Figure 11. Original (top) and processed (bottom) image of a laser engraved Coreno tile obtained with the system configuration in Figure 2 and in Table 1.

Monno in [57];

2. microscopic, where we want to characterize the engraving edge, in order to improve the cleanliness of the engraving, from which the contrast effect and the readability are a direct consequence.

Figure 11 shows an example of image obtained with the system described in § 4.2. The light stripes perpendicular to markings allow a three dimensional reconstruction of the border shape. A special peak-following algorithm has been developed to extract the surface profiles from such noisy images (laser speckle), without image pre-processing.
The laser speckle has an average size of 40 μm. The estimated system resolution is about 50 μm (before interpolation, for each profile in a grabbed image), so this method is not suitable for process characterization.
Conversely, optical profilometry has a sufficient resolution (Figure 10) for the validation of the artificial vision system.
Regarding the acquisition with the optical profilometer, the scanning of the (white) Carrara Marble has produced isolated scattering problems probably caused by the orientation of crystals of the same order of the profilometer spot size. In fact this effect is more frequent with the steepest marking surfaces.
Wrong profile samples (spikes) are easily detectable. They are less than 1% and are simply removed from the profile as outliers. If their number exceeds 1%, the acquisition is repeated.
Concurrent profilometer analysis of laser and abrasive waterjet markings will allow the definition of edge shapes as a function of the working parameters. Such shape information will improve the accuracy of the artificial vision system proposed (based on structured light) by interpolation of primitives, for on-line inspection of markings and engraving process control.

6.5 Characterization of abrasive waterjet processed (AWJ) surfaces

The integrated stylus/optical surface acquisition system developed described in § 5.1 has been designed having in mind rugged surfaces, according to our classification (§ 1.1).
Among all available samples, we have measured those that did not pose stylus measurement problems.
In the first part of our work, we have successfully validated the measurement of our optical profilometer with our stylus instrument (Table 2) following the scheme of Figure 1, as described here.
In order to compare the results, we have setup a Gaussian digital filter (DIN 4777) [55] in our Profile Analysis module (Figure 3), using the expression

$$G(z) = \frac{e^{-\pi\left(\frac{z}{\alpha\lambda_c}\right)^2}}{\alpha\lambda_c}$$

where

$$\alpha = \sqrt{\frac{\ln 2}{\pi}}$$

after subtracting the corresponding coordinates of the best-fit least-squares line.
The digital filter has been preliminarily validated by application to the unfiltered output profile coming from our stylus instrument and this result has been compared with the output of the software embedded in the stylus instrument.

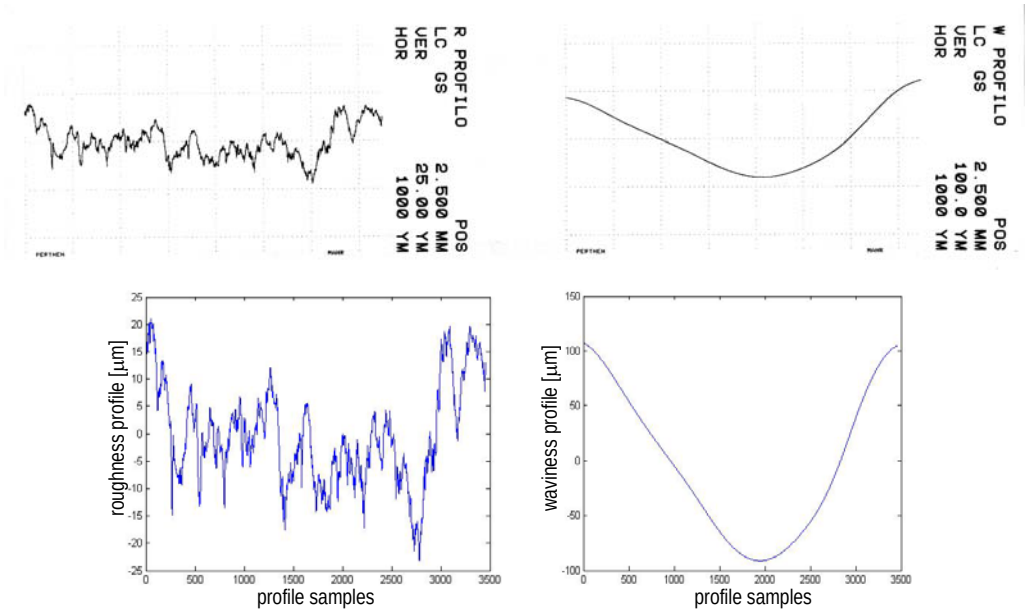

Figure 12. Visual validation of the Gaussian digital filter implemented. Top: direct output of our stylus instrument (Table 2) filtered by the embedded software, the roughness (left) and the waviness (right) profiles. Bottom: output of our Profile Analysis module (Figure 3) applied to the primary stylus profile.

In Figure 12, the processed results can be visually compared: the shapes of both the roughness and of the waviness profiles obtained with the two methods are practically coincident.
After assessing the correctness of profile filtering and best-fit line subtraction, we have designed an acquisition strategy by our optical profilometer synthesized in Table 3 for future analyses on rugged stone surfaces.
Our acquisition strategy has been tested on abrasive waterjet processed samples, provided by Annoni and Monno within [57].

Working conditions	*Sample n. 6*	*Sample n. 59*	*Sample n. 68*
Nozzle speed [mm/minute]	1000	2000	2000
Abrasive flow [g/minute]	50	150	150
Nozzle angle	0^o	0^o	45^o
Focalization diameter/Orifice diameter ratio	1.02	0.76	1.02

Table 4. The main parameters used for the abrasive waterjet processed surfaces analyzed in Table 5. The stone type is Pearly (Perlato) of Coreno in both cases. Samples have been provided by Annoni and Monno within [57].

In Table 5 the average roughness and the total waviness parameters Ra [19] and Wt [56] extracted from 20 profiles are compared. The scan direction is perpendicular to the waterjet nozzle direction.
As expected, the measurements of the two instruments are not significantly different and almost coincident in most acquisitions.
It should also be noticed that

- although the two instruments have been used on the same area, they do not scan exactly the same points,
- they use a different working principle, and
- the spot size/tip diameter (Table 2) of the two instruments are different.

This analysis validates the whole acquisition chain of the system developed for application to rugged stone surfaces.

Number of profiles	20
Spacing between profiles [mm]	0.5
Profile scan length [mm]	12.5
Cut wavelength λ_c [mm]	2.5
Evaluation length [mm]	3 x 2.5
Scan rate(*) [samples/s]	512
Translation speed(*) [mm/s]	0.8
Linear resolution(*) [samples/mm]	640

(*) Optical profilometer

Table 3. Acquisition strategy for the roughness parameters in Table 5. The profile evaluation length, and consequently the number of sampling intervals for the determination of the roughness parameters (3 instead of 5 as requested by [19]), is limited by the size of available samples.

From a preliminary analysis of the roughness parameters, the process under examination exhibits a high variability from zone to zone, as expressed by the standard deviation of both Ra and Wt (Table 5). Such variability is particularly relevant

	Optical profilometer				Stylus texture measuring instrument			
	Ra68	**Wt68**	**Ra6**	**Wt6**	**Ra68**	**Wt68**	**Ra6**	**Wt6**
1	8,31	270,06	17.74	169,42	7.51	136,20	23.1	226,00
2	9,09	269,65	19.00	210,60	6.77	74,58	11.99	168,20
3	7,68	267,89	15.28	185,10	7.45	70,28	20.39	161,10
4	7,81	239,36	17.17	185,39	6.65	48,13	15.23	135,20
5	6,69	169,18	19.37	191,98	6.26	51,97	21.09	231,70
6	6,46	123,10	28.57	206,07	6.32	66,80	23.01	249,20
7	7,29	127,41	12.05	160,45	6.62	167,60	17.88	192,00
8	8,07	173,66	17.37	173,81	8.12	199,90	17.85	188,40
9	8,25	179,37	16.53	185,00	7.11	293,50	29.02	164,80
10	7,17	161,50	17.37	212,10	6.47	232,00	23.35	131,20
11	6,00	186,10	18.82	215,13	5.62	103,70	19.23	103,60
12	7,02	240,58	17.68	204,82	5.07	39,31	24.44	158,00
13	8,66	251,75	19.36	213,30	5.43	140,80	18.68	185,10
14	9,42	247,75	19.47	268,32	7.57	154,70	18.16	238,00
15	11,23	261,01	15.91	205,42	6.32	128,40	22.86	234,90
16	8,85	217,34	23.06	198,63	6.77	217,00	22.64	237,20
17	7,68	177,50	27.30	173,57	9.98	291,40	20.94	162,10
18	8,14	91,45	22.34	136,90	8.82	221,20	16.72	189,70
19	6,64	42,76	18.93	74,46	7.51	140,00	24.32	155,90
20	6,52	61,17	19.18	154,22	6.9	141,00	22.34	230,20
$\bar{x}$	**7,85**	**187,93**	**19.12**	**186,23**	**6.96**	**145,92**	**20.66**	**187,13**
s	**1,24**	**70,65**	**3.83**	**38,44**	**1.14**	**77,33**	**3.81**	**41,93**

Table 5. Comparison between the roughness parameters obtained using our optical profilometer and our stylus texture measuring instrument (Table 2). The parameters Ra [19] and Wt [56] have been calculated from 20 acquisitions for the samples n. 6 and 68 (Table 4). The mean $\bar{x}$ and the standard deviation s of the data above are reported in the last two rows.

for the waviness, which is the desired surface effect obtained with the process under investigation.

A good discrimination ability among the different working conditions is also provided by Ra measured with the used λ_c.
An example of optically digitized surface is shown in Figure 13. The sampling parameters in Table 3 yield a correct surface representation and characterization.
This extensive data collection justifies the development of the automatic system described in § 5.1 for the correct acquisition of over 90 samples processed by AWJ in different conditions.

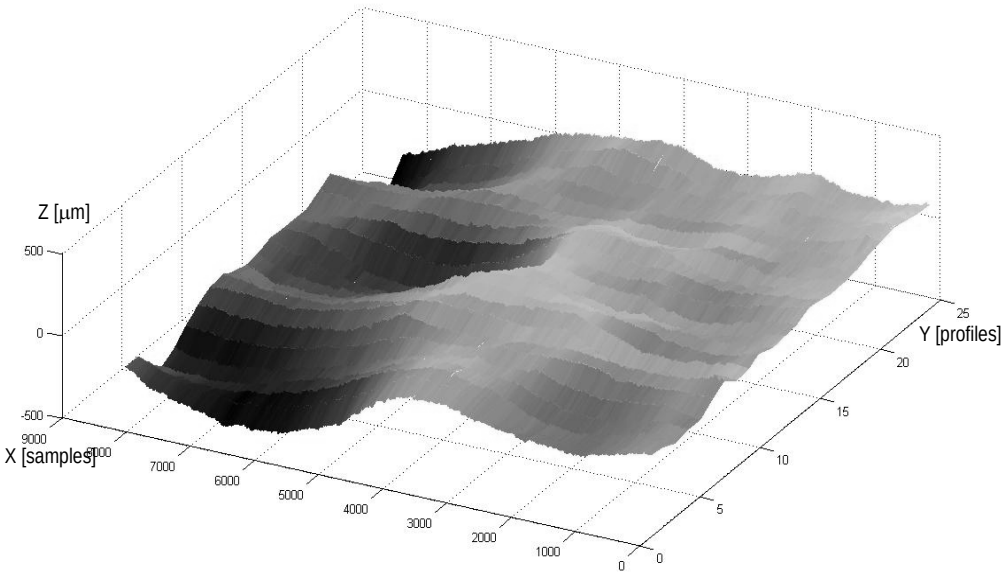

Figure 13. Three dimensional representation of 25 profiles of sample n. 59 (Table 4). The surface has been obtained as in Table 3.

7 CONCLUSIONS

An industrial perspective of the quality requirements in manufacturing of stone products has been presented and a classification of surface types has been proposed. For each class, (few) methods available in the literature have been critically reviewed. Innovative methods have been proposed and described in this paper:

- we have presented a reflectometer (being patented) and the use of Rk for roughness measurement on polished stone surfaces;
- we have approached the analysis of laser and abrasive waterjet engraved

surfaces using optical profilometry for edge characterization and artificial vision with structured light for the three dimensional on-line inspection;
- we have approached the analysis of abrasive waterjet processed surfaces by optical profilometry.

7.1 Research opportunities for stone surface analysis by optical methods

From our analysis it can be concluded that a single device today is not sufficient for all stone surface inspection needs, but most problems can be approached by optical methods. Their application seems more a market than a technological problem. However under a research perspective a lot of work can be done.
The advantages of faster non-contact surface assessment and increased inspection area make them suitable for on-line application, for inspection on the final product and also at intermediate stages for process control.
The benefit of a single optical technology for most stone surface inspection requirements can also be investigated.
In this regard, artificial vision seems the best candidate.
The benefit of having only one system needs to be compared with the drawback of managing its complexity and the possibility of optimizing individually different solutions.
Consolidated optical methods to be investigated for stone surface application as a concrete research and industrial opportunity, include, but are not limited to: optical followers (Newton, Hadamard, obstructions, Foucault), interference e differential interference, amplitude division, depth of focus, division of wavefront, fringes of equal chromatic order, heterodyne, holography, hybrid microscope, Moiré, Nomarski, oblique angle, polarization, phase detection, focussed spot, interferometry (Mirau), scatter (phase/amplitude/polarization/position/angle), fractal, autocorrelation, multiple reflection, ray tracing, Gaussian speckle).
As a direct consequence, the lack of standards in the stone industry is still a limitation and requires more research.

ACKNOWLEDGEMENTS

This work was co-sponsored by the Italian Ministry of University and Research [57].
It is also based on the final projects of the following undergraduate mechanical engineering students (in alphabetical order):
- Mr. Alessandro Bernardelli and Mr. Guido Lenzi (characterization of rugged stone surfaces),
- Mr. Daniele Ciomei (3D reconstruction by stereo vision),
- Mrs. Federica Fanti (acquisition of rugged stone surfaces by structured light),
- Mr. Alessandro Maggesi (engineering of the reflectometer),
- Mr. Camillo Scionti (characterization of smooth stone surfaces),
- Mr. Valerio Zambardi (setup of an integrated NC stylus/optical surface acquisition system).

Dr. Santo Gentile from GDTech snc (Pisa) is acknowledged for glossmeter and reflectometer experimental tests and for the realization of prototypes.
Polished and part of laser engraved samples have been provided by the Department of Industrial Engineering, University of Cassino, under [57].
Waterjet processed and engraved samples have been provided by the Department of Mechanics, Politecnico di Milano, under [57].
Spectrographic tests on stones have been supported by Diessechem srl (Milan).

REFERENCES

[1] ISO 8785:1998. Geometrical Product Specification (GPS) - Surface imperfections - Terms, definitions and parameters.

[2] Lanzetta, M., Tantussi, G., 1997, The quality control of natural materials: defect detection on Carrara marble with an artificial vision system, 3rd Aitem Conference, Fisciano (SA), Italy, September 17-19, 1997, pp. 449-456.

[3] Tantussi, G., Lanzetta, M., Santochi, M., 1995. The quality control in the field of marble: an artificial vision system for the automatic selection of tiles, Proceedings of the 2nd A.I.Te.M Conference, Italian Association of Mechanical Technology, Padua (Italy), September 18th-20th, 1995, pp. 439-448.

[4] Lee, J.R.J., Smith, M.L., Smith, L.N., Midha, P.S., December, 2005. Robust and efficient automated detection of tooling defects in polished stone, Computers in Industry, v 56, n 8-9, Machine Vision, pp. 787-801.

[5] Hsu, J.-P., Fuh, C.-S., 1995. Image segmentation for stone-size inspection, Proceedings of SPIE - The International Society for Optical Engineering, v 2501/3, pp. 1614-1625.

[6] Garceran Hernandez, V., Clemente Perez, P., Garcia Perez, L.G., Tomas Balibrea, L.M., Puyosa Pina, H., 1995. Traditional and neural networks algorithms: applications to the inspection of marble slab, Proceedings of the IEEE International Conference on Systems, Man and Cybernetics, v 5, pp. 3960-3965.

[7] Lonardo, P. M., Lucca, D. A., De Chiffre, L., 2002. Emerging Trends in Surface Metrology, Annals of the CIRP, 51/2/2002, pp. 701-723.

[8] Schwenke, H., Neuschaefer-Rube, U., Pfeifer, T., Kunzmann, H., 2002. Optical Methods for Dimensional Metrology in Production Engineering, Annals of the CIRP 51/2/2002, pp. 685-699.

[9] De Chiffre, L., Lonardo, P.M., Trumpold, H., Lucca, D.A., Goch, G., Brown, C.A., Raja, J., Hansen, H.N., 2000. Quantitative characterisation of surface texture, Annals of the CIRP, 49/2, pp. 635-652.

[10] Hocken, R.J., Chakraborty, N., Brown, C., 2005. Optical Metrology of Surfaces, 54/2/2005, pp. 705-720.

[11] Whitehouse, D. J., Bowen, D. K., Venkatesh, V. C., Lonardo, P., Brown, C. A., 1994. Gloss and Surface Topography, Annals of the CIRP 43(2), p. 541-549.

[12] Schwenke, H., Neuschaefer-Rube, U., Pfeifer, T., Kunzmann, H., 2002. Optical Methods for Dimensional Metrology in Production Engineering, Annals of the CIRP 51/2, p. 685.

[13] Whitehouse, D.J., 1994. Handbook of Surface Metrology, Institute of Physics Publishing, Bristol, Philadelphia, ISBN 0-7503-0039-6.

[14] Huang, H., Li, Y., Shen, J.Y., Zhu, H.M., Xu, X.P., October 2002. Micro-structure detection of a glossy granite surface machined by the grinding process, Journal of Materials Processing Technology, Volume 129, Issues 1-3, 11, pp. 403-407.

[15] Xi, F., Zhou, D., 2005. Modeling surface roughness in the stone polishing process, International Journal of Machine Tools and Manufacture, v 45, n 4-5, pp. 365-372.

[16] Dai, Q.L., Qin, C.Q., Xu, X.P., 2006. Study on the dependence of glossiness on the micro-uneven of natural, Key Engineering Materials, v 304-305, Advances in Grinding and Abrasive Technology XIII, pp. 305-309.

[17] Bonifazi, G., Marinelli, S., 2003. Ornamental stone finished product aesthetic inspection and characterization through a digital spectrophotometric approach, Proceedings of SPIE - The International Society for Optical Engineering, v 5011, 2003, pp. 243-250.

[18] Avdelidis, N. P., Delegou, E. T., Almond, D. P., Moropoulou, A., October 2004. Surface roughness evaluation of marble by 3D laser profilometry and pulsed thermography, NDT & E International, Volume 37, Issue 7, pp. 571-575.

[19] ISO 4287:1997 Ed. 1 + Corrigenda 1 (1998) & 2 (2005) Geometrical Product Specifications (GPS) -- Surface texture: Profile method -- Terms, definitions and surface texture parameters.

[20] ASTM D 523-94, 1999. Standard Test Method for Specular Gloss, 5.1. pp. 1.

[21] H. K. Hammond, I. Nimerroff, ANNO??? Measurement of sixty Degree Specular Gloss, Journal of Research, Nat. Bureau Standards.

[22] ASTM E 430-97, 1997. Measurement of the surface brightness by goniofotometry, pp. 727-739.

[23] ISO 2813, 1997. Paints and varnishes: determination of specular gloss of non-metallic paint films at 20/60/85 degrees.

[24] ASTM C346-87, 2004 Standard Test Method for 45-deg Specular Gloss of Ceramic Materials.

[25] Nimeroff, I., Hammond, H.K., Richmond, J.C., Crandall, J.R., 1956. Specular-Gloss Measurement of Ceramic Materials, Journal of the American Ceramic Society 39 (3), 103–109.

[26] Born, M. and Wolf, E. Principles of Optics, Electromagnetic Theory of Propagation, Interference, and Diffraction of Light, 7th ed. Cambridge, England: Cambridge University Press, 1999.

[27] Obein, G., Knoblaugh, K., Vienot, F., 2004. Difference scaling of gloss: Nonlinearity, binocularity, and constancy, Journal of Vision, vol. 4, pp. 711-720.

[28] White, D.R., Saunders, P., Bonsey, S.J., van de Ven, J., Edgar, H., 1998. Reflectometer for measuring the bidirectional reflectance of rough surfaces, Applied Optics vol. 37, No. 16, pp. 3450-3454.

[29] Otremba, Z., 2004. Modelling the bidirectional reflectance distribution function (BRDF) of seawater polluted by an oil film, Optics Express, vol 12 n.8, pp. 1671-1676.

[30] Nadal, M.E., Ambler Thompson, E., 2001. NIST Reference Goniophotometer for Specular Gloss Measurements, Optical Technology Div. Vol. 73, No. 917 pp. 73-80.

[31] Benavente, D., Martinez-Verdu, F., Bernabeu, A., Viqueira, V., Fort, R., Garcia del Cura, M. A., Illueca, C., Ordonez, S., October, 2003. Influence of Surface Roughness on Color Changes in Building Stones, Color Research and Application, v 28, n 5, pp. 343-351+323-324, ISSN 0361-2317.

[32] Fort, R., Mingarro, F., López de Azcona, M.C., Rodriguez Blanco, J., December 2000. Chromatic parameters as performance indicators for stone cleaning techniques, Color Research & Application, Volume 25, Issue 6, pp. 442-446.

[33] Azriel Rosenfeld, A, 01/04/1999. Image Analysis and Computer Vision, Computer Vision and Image Understanding, Volume 74, Issue 1, pp. 36-95 doi:10.1006/cviu.1999.0746

[34] Oral, A., Erzincanli, F., March/April, 2004. Computer-assisted robotic tiling of mosaics, Robotica, v 22, n 2, pp. 235-239.

[35] Lanzetta, M., Gentile, S., Tantussi, G., Rizzello, F., Coluccia, M., Gaggio, G., 2006. Computer-aided pre-installation for stone slabs, Marmo Macchine Classic, n. 190, vol. 36, pp. 102-112.

[36] Ayache, N., 1991. Artificial Vision for Mobile Robots, The MIT Press, Cambridge Massachusetts, London England.

[37] Mohan, R., Medioni, G., Nevatia, R., Feb. 1989. Stereo error detection, correction, and evaluation, Pattern Analysis and Machine Intelligence, IEEE

Transactions on, Volume 11, Issue 2, pp. 113–120, Digital Object Identifier 10.110934.16708.

[38] Ahuja, N., Abbott, A.L., Oct. 1993. Active stereo integrating disparity, vergence, focus, aperture and calibration for surface estimation, Pattern Analysis and Machine Intelligence, IEEE Transactions on, Volume 15, Issue 10, pp. 1007–1029, Digital Object Identifier 10.110934.254059.

[39] Maitre, H., Luo, W., Feb. 1992. Using models to improve stereo reconstruction, Pattern Analysis and Machine Intelligence, IEEE Transactions on, Volume 14, Issue 2, pp. 269-277, Digital Object Identifier 10.110934.121794.

[40] Chichyang C., Zheng, Y.F., June 1995. Passive and active stereo vision for smooth surface detection of deformed plates, Industrial Electronics, IEEE Transactions on, Volume 42, Issue 3, pp. 300–306, Digital Object Identifier 10.110941.382141.

[41] Albrecht, P., Michaelis, B., Feb. 1998. Improvement of the spatial resolution of an optical 3-D measurement procedure, Instrumentation and Measurement, IEEE Transactions on, Volume 47, Issue 1, pp. 158-162, Digital Object Identifier 10.110919.728810.

[42] Huang, C.-C., Zheng, Y.F., June 1996. Integration of vision and laser displacement sensor for efficient and precise digitizing, Industrial Electronics, IEEE Transactions on, Volume 43, Issue 3, pp. 364 – 371, Digital Object Identifier 10.110941.499808.

[43] Cochran, S.D., Medioni, G., Oct. 1992. 3-D surface description from binocular stereo, Pattern Analysis and Machine Intelligence, IEEE Transactions on, Volume 14, Issue 10, pp. 981–994, Digital Object Identifier 10.110934.159902.

[44] Nurre, J.H.; Hall, E.L., Dec. 1992. Encoded moire inspection based on a computer solid model, Pattern Analysis and Machine Intelligence, IEEE Transactions on, Volume 14, Issue 12, pp. 1214-1218, Digital Object Identifier 10.110934.177388.

[45] Del Taglia, A., Paolucci, A., 1995. The shadow-Moiré method applied to 3D model copying, Annals of the Cirp, vol 44, n 1, pp. 497-500.

[46] Fieguth, P.W., Staelin, D.H., 01/02/1994. High-accuracy profiler that uses depth from focus, Applied Optics, v 33, n 4, pp. 686-689.

[47] Ramana, K. V., Ramamoorthy, B., 1996. Statistical methods to compare the texture features of machine surfaces, Pattern Recognition 29, 9, pp. 1447–1459.

[48] Priya, P., Ramamoorthy, B., March 2007. The influence of component inclination on surface finish evaluation using digital image processing,

International Journal of Machine Tools and Manufacture, Volume 47, Issues 3-4, pp. 570-579.

[49] Carrino, L., Monno, M., Polini, W., Turchetta, S., 2002. Surface processing of natural stones through AWJ, 16th International Conference on Water Jetting, Aix en Provence, France, October 16-18, 2002.

[50] Carrino, L., Polini, W., Turchetta, S., Monno, M., 2003. Bending radius dependance in AWJ machining of stone free-form profiles, WJTA American Waterjet Conference, Houston (Texas), 17-19 Aug. 2003, pp. 1-15.

[51] Ravasio, C., Monno, M., 2003. Erosion of natural stone by abrasive grains, WJTA American Waterjet Conference, Houston (Texas), 17-19 Aug. 2003, pp. 1-12.

[52] ISO 1073-1:1976. Ed. 1, Alphanumeric character sets for optical recognition -- Part 1: Character set OCR-A -- Shapes and dimensions of the printed image.

[53] ISO 1073-2:1976. Ed. 1, Alphanumeric character sets for optical recognition -- Part 2: Character set OCR-B -- Shapes and dimensions of the printed image.

[54] ISO 1004:1995. Information processing - Magnetic ink character recognition - Print specifications.

[55] Tantussi, G., Santochi, M. 1992. Impiego dei filtri digitali nella misura della rugosità, Rassegna di Meccanica n. 9, pp. 386-391.

[56] NF E 05-015, 12/1982. Etats de surface des produits. Prescriptions, généralités, terminologie, définitions. AFNOR France.

[57] National Interest Research Project (PRIN) 2004, DM 30 (12/02/2004) “Inspecting the Surfaces of Natural Stone Products”, protocol: 2004093934. http://cofin.cineca.it.